Study On Stellite 6 Overlay Welding on Super Duplex Stainless Steel by Plasma Transfered Arc Welding

H. Yasin[1], S. Dhanalakshmi[2] and D. Noorullah[3]
[1]*PG Student, Department of Metallurgical Engineering, Government College of Engineering, Salem-11*
[2]*Assistant Professor (Sr.Gr), Department of Metallurgical Engineering, Government College of Engineering, Salem-11*
[3]*Head of the Department, Department of Metallurgical Engineering, Government College of Engineering, Salem-11*

Abstract: **The long-term service performance of Stellite 6 overlays on Super Duplex Stainless Steel (UNS S32760) is significantly hindered by embrittlement and crack formation. These issues stem from Fe diffusion into the overlay, which results in brittle phase formation, including sigma (σ) phases and Cr-rich carbides, leading to hardness variations and stress concentrations. This study explores the introduction of Inconel 625 as a buffer layer between the SDSS substrate and the Stellite 6 overlay to mitigate these challenges. Inconel 625, with its high nickel content and exceptional thermal stability, minimizes dilution effects, stabilizes the microstructure, and prevents the formation of brittle phases. Through microstructural analysis, mechanical testing, and phase evaluations, this research demonstrates that the buffer layer effectively reduces crack susceptibility, enhances toughness, and ensures the weldment's durability under harsh service conditions. This solution not only improves performance but also extends the service life of industrial components in high-temperature and high-pressure environments.**

Keywords: **PTAW, Super Duplex Stainless Steel, Stellite 6, Inconel 625, Buffer Layer, Crack Mitigation, Hardfacing, Overlay Welding**

1. INTRODUCTION

Super Duplex Stainless Steel (SDSS) is an advanced form of duplex stainless steel combining austenitic and ferritic microstructures with elevated levels of chromium, molybdenum, and nitrogen for enhanced corrosion resistance and strength. However, when Stellite 6, a Co-Cr based hardfacing alloy, is directly applied on SDSS, Fe diffusion during service can cause the formation of brittle intermetallic phases such as σ-phase and Cr-rich carbides. These microstructural issues cause embrittlement, crack propagation, and eventually lead to failure. Inconel 625, a Ni-Cr-Mo alloy, acts as a stable buffer layer that reduces dilution, minimizes Fe diffusion, and prevents phase imbalance. This project investigates the use of Inconel 625 buffer layers under Stellite 6 overlays deposited using Plasma Transferred Arc Welding (PTAW) on UNS S32760 SDSS rings to analyze improvements in weld structure and performance.

2. LITERATURE REVIEW

Extensive studies have been conducted to examine the challenges of overlaying Stellite 6 directly on SDSS. Jiankun Xiong et al. identified brittle phase formation due to Fe diffusion. Deshmukh et al. reviewed PTAW as an efficient coating process, while Lorenzoni et al. emphasized the influence of dilution on corrosion resistance in Inconel 625 overlays. Researchers such as Fande and Rozmus-Górnikowska demonstrated improved properties in welds using Inconel interlayers. Multiple researchers have used SEM, EDS, and XRD analyses to study microstructural evolution. Key issues addressed in past studies include sigma phase formation, dilution control, crack resistance, and phase balance. This project builds on these studies by incorporating a controlled PTAW process to examine the dual-layer system of Inconel 625 and Stellite 6 on SDSS.

3.EXPERIMENTAL PROCEDURE

The methodology includes literature review, material selection, welding setup, process execution, and post-weld testing. Materials - Base Material: Super Duplex Stainless Steel (UNS S32760) –

Table 3.1 shows its composition.

Element	Percentage (%)
Carbon (C)	≤ 0.03
Chromium (Cr)	24.0–27.0
Nickel (Ni)	4.5–6.5
Molybdenum (Mo)	2.5–3.5
Nitrogen (N)	0.20–0.30
Manganese (Mn)	≤ 1.5
Silicon (Si)	≤ 0.8
Phosphorus (P)	≤ 0.03
Sulfur (S)	≤ 0.02
Iron (Fe)	Balance

Buffer Layer: Inconel 625 (ERNiCrMo-3) –

Table 3.2 shows its composition.

Element	Percentage (%)
Nickel (Ni)	≥ 58.0
Chromium (Cr)	20.0–23.0
Molybdenum (Mo)	8.0–10.0
Iron (Fe)	≤ 5.0
Niobium (Nb)	3.15–4.15
Manganese (Mn)	≤ 0.50
Silicon (Si)	≤ 0.50
Carbon (C)	≤ 0.10
Phosphorus (P)	≤ 0.015
Sulfur (S)	≤ 0.015

Final Overlay: Stellite 6 (ERCoCr-A) –

Table 3.3 shows its composition.

Element	Percentage (%)
Carbon (C)	0.9 – 1.4
Manganese (Mn)	1
Silicon (Si)	2
Chromium (Cr)	26-32
Nickel (Ni)	3
Molybdenum (Mo)	1
Iron (Fe)	3
Tungsten(W)	3-6
Cobalt (Co)	Balance
Others	0.5

Problem Identification The direct application of Stellite 6 on SDSS results in elemental diffusion, brittle phase precipitation, thermal mismatch, and crack propagation. These lead to poor weld reliability. Hence, Inconel 625 is used as a buffer layer.

Process Details Welding was performed using a PTAW machine at Charvi Ring Products, Coimbatore. PTAW used a non-consumable 4 mm tungsten electrode with 2% thorium and high-purity argon gas. The base material (25 mm thick, 210 mm diameter SDSS ring) was cleaned using liquid penetrant inspection before welding.

Welding Data 1st Layer (Buffer - Inconel 625): 130 A, 23–24 V, 12–15 g/min, 1.5 mm thickness. 2nd Layer (Overlay - Stellite 6): 116 A, 23–24 V, 12–15 g/min, 1.5 mm thickness. Preheat Temp: 52°C | Interpass Temp: 176°C | Travel Speed: ~156 mm/min. Shielding Gas: Argon (99.997%)

Fig. 3.1: Weld Model Diagram

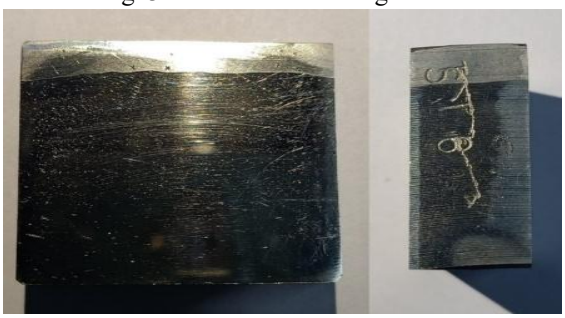

Fig. 3.2: Test Specimen

4. RESULTS AND DISCUSSION

4.1 Chemical Analysis

Element	Spec (%)	Actual (%)
Carbon (C)	0.9 – 1.4	1.011
Manganese (Mn)	1	0.291
Silicon (Si)	2	1.454
Chromium (Cr)	26-32	30.791
Nickel (Ni)	3	6.500
Molybdenum (Mo)	1	-
Iron (Fe)	3	-
Tungsten(W)	3-6	3.752
Cobalt (Co)	Balance	49.919
Phosphorus (P)	-	0.011
Sulphur (S)	-	0.004

Table 4.1 (Table 4.1) confirms that key elements like Cr, Co, and W are present within specification. Fe and Mo values were closely monitored. Fig. 4.1 shows elemental distribution.

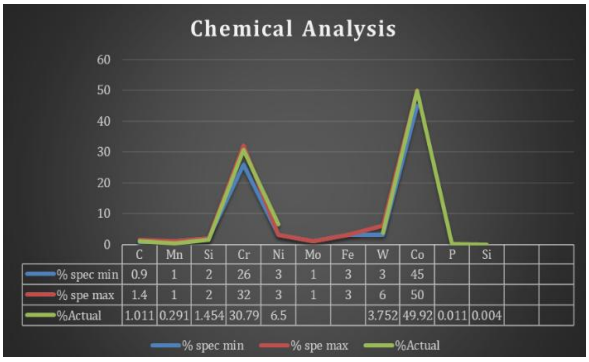

	C	Mn	Si	Cr	Ni	Mo	Fe	W	Co	P	Si
% spec min	0.9	1	2	26	3	1	3	3	45		
% spe max	1.4	1	2	32	3	1	3	6	50		
%Actual	1.011	0.291	1.454	30.79	6.5			3.752	49.92	0.011	0.004

Fig 4.1: Chemical Analysis Graph

4.2 Hardness Analysis

4.2.1. Rockwell Hardness Test

Test Method: ASTM E18:2022

Test Location – On Weld 3.5 mm from Base Metal

Rockwell Hardness Values (HRC):

43,45,45Avg: 44.33 HRC

The Rockwell Hardness Test Shows that the overlay stellite 6 HRC is above 36 and below 45. This proves the effectiveness of the process.

4.2.2. Vickers's Hardness Test

Vickers's hardness testing machine was used to measure the hardness as per ASTM E92:2023 of the weld metal with a 10 Kg load. The hardness survey conducted various positions as per the Fig 4.2. In each location hardness survey conducted at 3 points and the hardness meets with the NACE MR0175: 2021/ISO 15156-2020. The survey conducted on the location as per the Fig 4.2 and the results are presented in Table 3.2

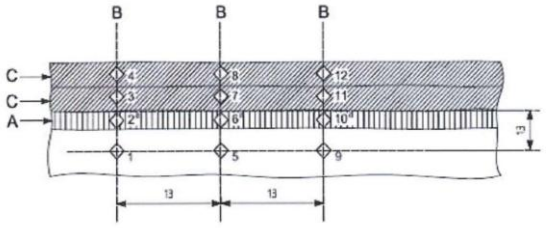

Fig 4.2: Survey Location

Table 4.2: Hardness Survey

Position	Indent location	Hardness value 1	Hardness value 2	Hardness value 3	Avg. Hv
Overlay top ST-6	4, 8, 12	388	403	370	387
Buffer Layer In 625	3, 7, 11	323	336	311	323
Base UNS S32760	1,5,9	295	297	300	297
HAZ (0.5 mm from fusion zone)	2,6,10	277	274	267	273

From fig 4.3, it is clearly shows that the hardness values of the weld top is better than parent metal indicating higher strength of the weld overlay.

Fig 4.3: Hardness Survey Graph

4.3. MACROSTRUCTURE ANALYSIS

Macro examination conducted on the specimen by using 7 x magnifications is referred in Fig 4.4. The sample was macro etched (Etchant – Glyceregia Reagent) and Macro examination of the weld specimen did not reveal any cracks, porosity or any other weld defects. Observed complete weld fusion in all examined area.

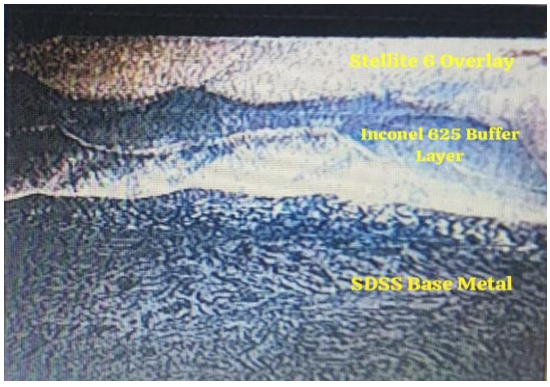

Fig 4.4: Macro Structure (x7 mag)

4.4. MICROSTRUCTURE ANALYSIS

Test Method: ASTM A923, Magnification: 100X

Etchant: 10% Oxalic acid & NaOH – Electrolytic etchant

Observation:

- Micro examination of the specimen revealed ferrite and austenite phase. The structure is free from intermetallic phases (like sigma, chi, laves) & other precipitates (Nitrides and carbides).
- Micro examination of the HAZ region did not reveal any cracks, porosity or any other defects.
- Micro examination of the weld region revealed inter dendritic structure present in the Cobalt solution.

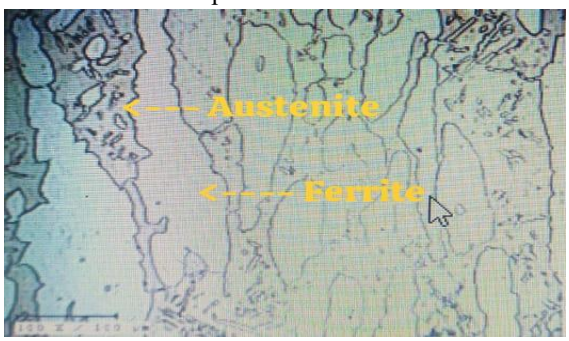

Fig 4.5: Base Metal - Mag: 100x

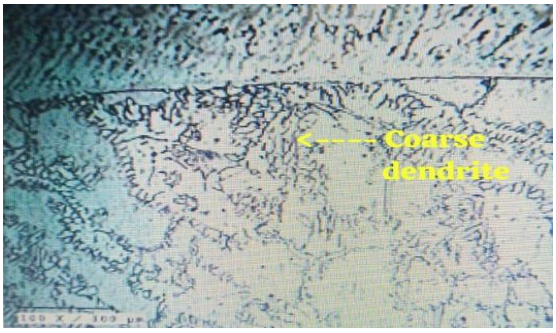

Fig 4.6: HAZ – Mag: 100x

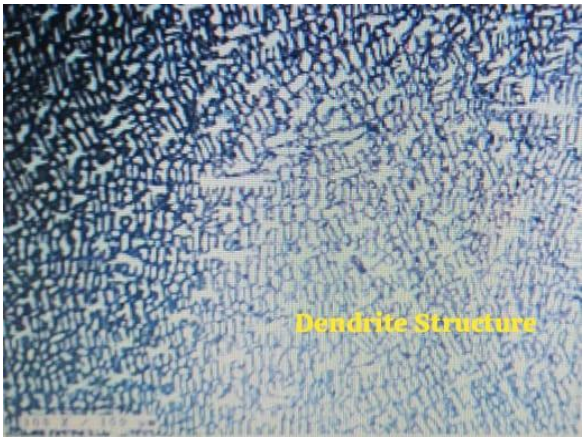

Fig 4.7: Weld – Mag: 100x

4.5 SEM and EDS Analysis

Scanning Electron Microscopy (SEM). SEM was used to examine the morphology and integrity of the overlay, heat-affected zone (HAZ), and interface regions.

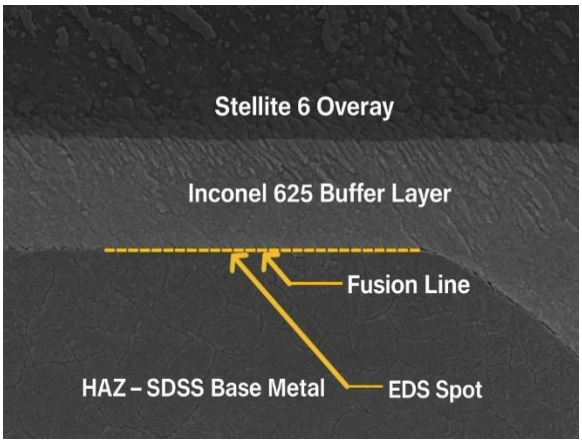

Fig. 4.8: the SEM survey locations across the weldment.

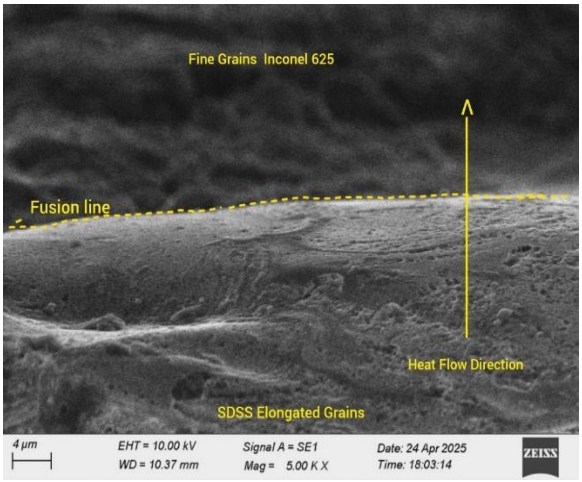

Fig 4.9: Fusion Line – SDSS and Inconel 625

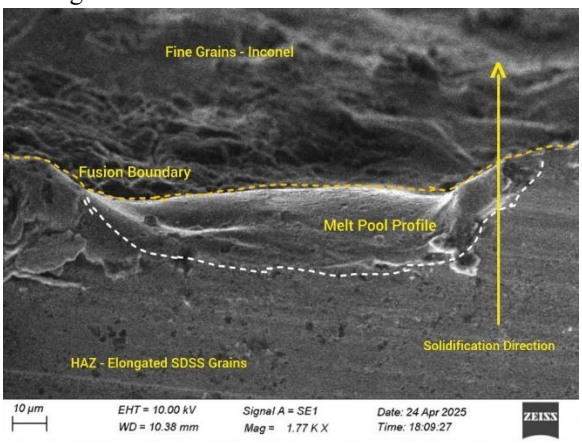

Fig 4.10: Alternate Fusion Line – SDSS and Inconel 625

Fig. 4.9–4.10 display the fusion line between SDSS and Inconel 625, revealing a clear boundary with minimal elemental mixing.

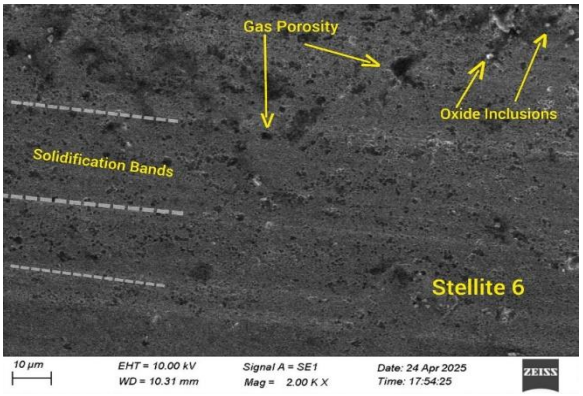

Fig 4.11: Cladding Surface – Stellite 6

Fig. 4.11 presents the cladding surface of Stellite 6, showing a refined dendritic microstructure, indicating uniform solidification.

Fig. 4.12–4.14 depict HAZ at varying magnifications. These reveal the absence of major porosity or cracking. Minor carbide precipitation was observed near the interface but within acceptable limits.

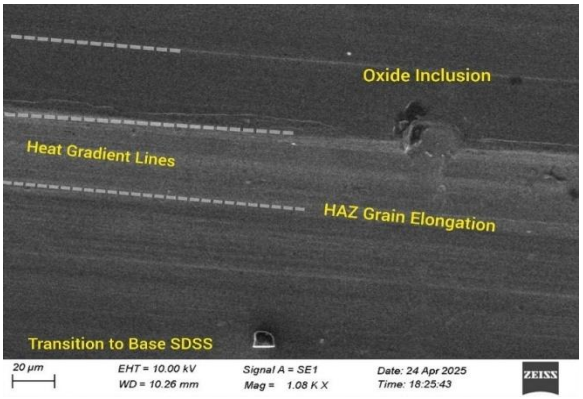

Fig 4.12: HAZ (Low Magnification)

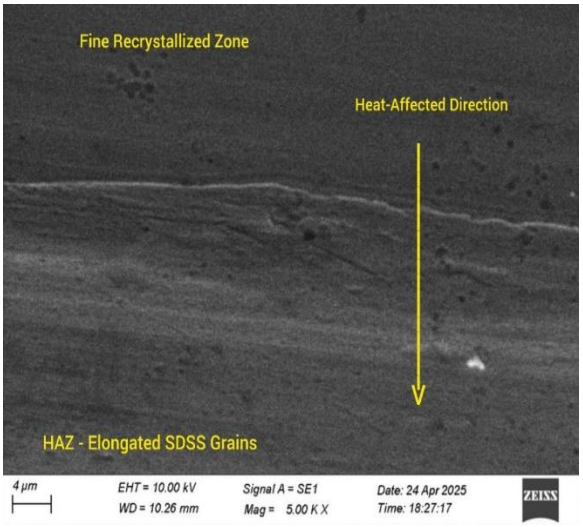

Fig 4.13: HAZ Interface (High Magnification)

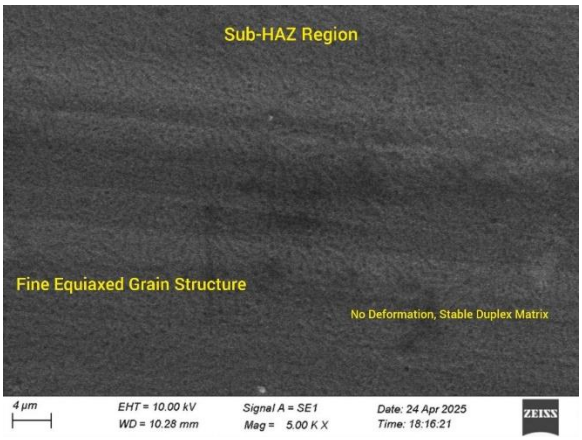

Fig 4.14: Deep HAZ / Sub-HAZ

The SEM analysis confirms:

- Minimal porosity
- Directional solidification at fusion lines
- Reduced interfacial cracking due to the Inconel 625 buffer
- A smooth transition from SDSS → Inconel → Stellite

Sharp and defect-free fusion line between SDSS and Inconel 625. Grain elongation in HAZ confirms controlled thermal gradient without structural break down. Stellite 6 overlay exhibited fine dendritic matrix with uniform solidification. No cracks, porosity, or secondary intermetallic phases detected in any region. Sub-HAZ region preserved duplex structure with equiaxed grains.

Energy Dispersive X-ray Spectroscopy (EDS)

EDS spot and mapping analyses were conducted to determine elemental distribution across the weld zones.

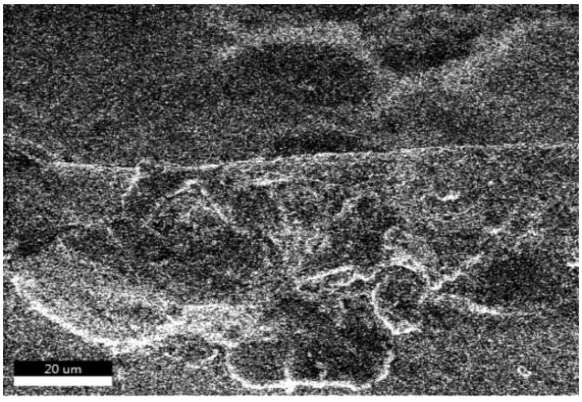

Fig. 4.15 shows the EDS spot locations.

Fig. 4.16–4.17 shows EDS elements overlay.

Fig 4.16: EDS Element Overlay

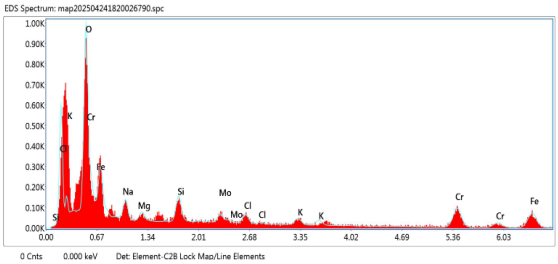

Fig 4.17: EDS Spectrum Graph

Figs. 4.18–4.26 provide distribution maps for Cr, Fe, O, Na, Mg, Si, Mo, Cl, and K.

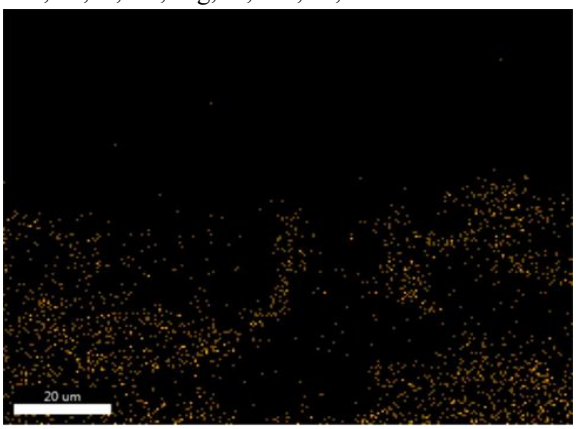

Fig 4.19: EDS Iron (Fe)distribution map

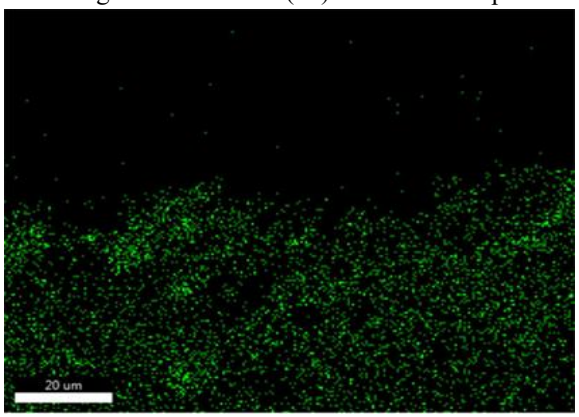

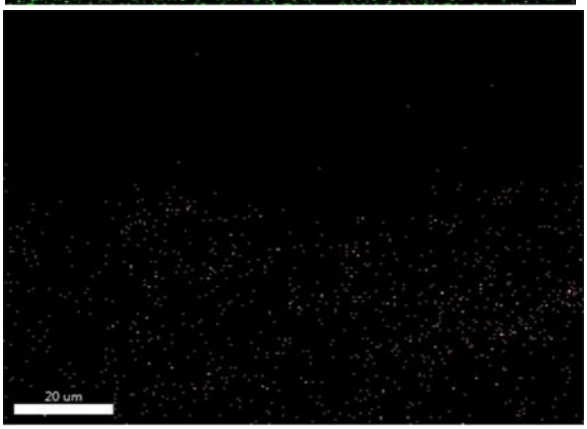

Fig 4.20: EDS Oxygen (O) distribution map

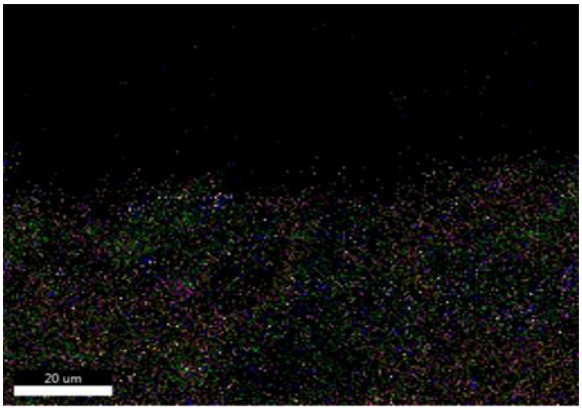

Fig 4.22: EDS Magnesium (Mg) distribution map

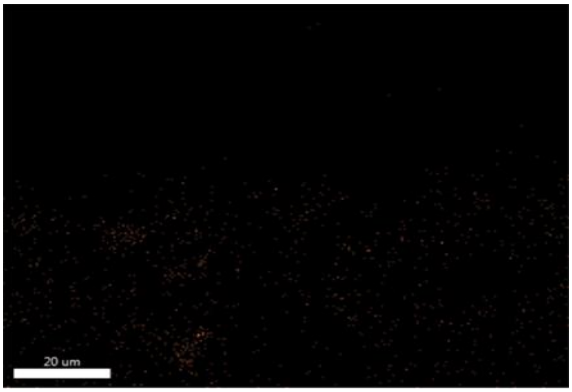

Fig 4.23: EDS Silicon (Si) distribution map

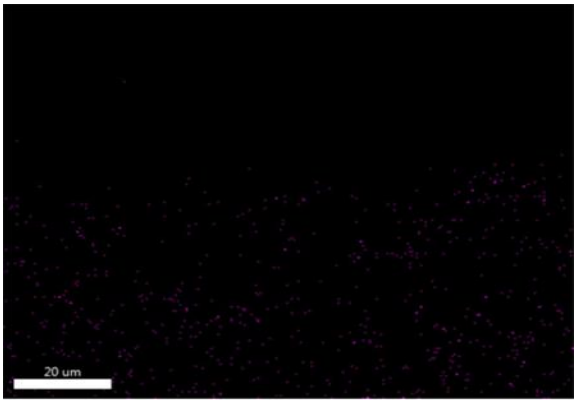

Fig 4.24: EDS Molybdenum (Mo) distribution map

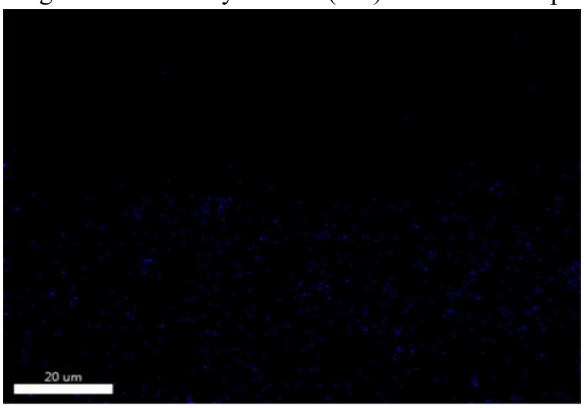

Fig 4.25: EDS Chlorine (Cl) distribution map

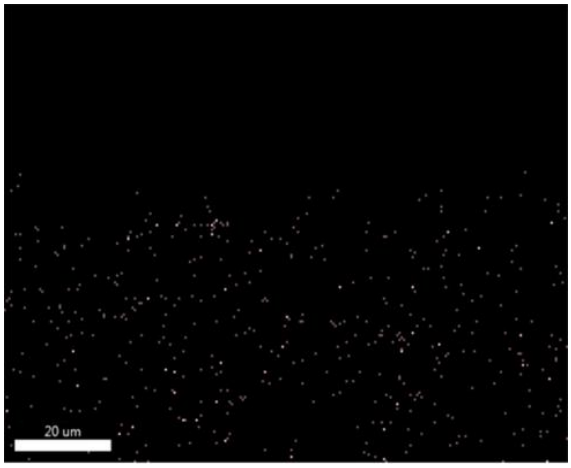

Fig 4.26: EDS Potassium (K) distribution map

Fig 4.21: EDS Sodium (Na) distribution map

Key Findings:
Iron (Fe): Diffusion from SDSS into the overlay was significantly reduced due to the Inconel 625 buffer.
Chromium (Cr): Uniformly distributed in the Stellite 6 overlay, contributing to corrosion resistance.
Cobalt (Co): Present as the matrix in the Stellite 6 overlay.
Nickel (Ni): Predominantly in the Inconel 625 layer, promoting microstructural stability.
Molybdenum (Mo): Detected in Inconel 625 and contributes to pitting resistance.
Oxygen (O): Trace surface oxides observed; no internal oxidation.
The EDS mapping confirms a smooth elemental gradient and excellent compositional stability, supporting the effectiveness of Inconel 625 as a buffer.

5.CONCLUSION

This study successfully demonstrated the effectiveness of using an Inconel 625 buffer layer in Plasma Transferred Arc Welding (PTAW) for depositing Stellite 6 overlays on Super Duplex Stainless Steel (UNS S32760). The direct deposition of Stellite 6 onto SDSS typically results in the formation of brittle phases (e.g., sigma phase and Cr-rich carbides), along with cracking due to Fe diffusion and thermal mismatch. By introducing Inconel 625 as a buffer, these problems were significantly reduced.

The SEM analysis showed refined and defect-free microstructures across the fusion lines. EDS mapping confirmed the controlled dilution of Fe and uniform distribution of critical alloying elements (Cr, Co, Ni, Mo), which contributed to enhanced corrosion and wear resistance. Hardness tests revealed values between 400–600 HV in the overlay region, verifying excellent mechanical integrity and surface hardness.

The addition of the Inconel 625 buffer layer minimized elemental mixing, stabilized the interface, reduced crack propagation, and improved toughness. These results validate the dual-layer overlay system as a superior approach for improving the service life and reliability of SDSS components used in extreme environments, such as oil and gas, marine, and chemical processing industries.

REFERENCE

[1] Xiong, J., Nie, F., Zhao, H., Zheng, L., Luo, J., & Wen, Z. (2019). Microstructure Evolution and Failure Behavior of Stellite 6 Coating on Steel after Long-Time Service. Coatings.

[2] Xu, L., Han, Y., Zhang, Y., Jing, H., & Zhao, L. (2020). Microstructure and Corrosion Studies on Different Zones of Super Duplex Stainless Steel UNS S32750 Weldment. Frontiers in Materials.

[3] Deshmukh, D. D., &Kalyankar, V. (2020). Recent Advances in PTA Welding for Hardfacing Applications. Materials Science Reports.

[4] Czupryński, A. (2019). Research on 16Mo3 steel pipe overlaid with superalloys Inconel 625 using robotized PPTAW. Welding Technology Review.

[5] Rozmus-Górnikowska, M., Blicharski, M., & Kusinski, J. (2014). Influence of weld overlaying methods on microstructure and

chemical composition of Inconel 625 boiler pipe coatings. Materials and Design.

[6] Fande, A. W., Kavishwar, S., Tandon, V., Narayane, D. C., & Bandhu, D. (2024). Influence of Inconel interlayer on microstructural, mechanical, and electrochemical characteristics in single-pass ATIG welding of dissimilar stainless steels. Materials Research Express.

[7] Guo, L., Xiao, F., Wang, F., Wei, W., & Luo, F. (2021). Influence of heat treatments on microstructure, mechanical properties, and corrosion resistance of Inconel 625 overlay cladded using PTIG. Materials Research Express.

[8] Guo, L., Xiao, F., Wang, F., Wei, W., & Luo, F. (2020). Effect of Heat Treatment Temperatures on Microstructure and Corrosion Properties of Inconel 625 Weld Overlay Deposited by PTIG. Materials Research Express.

[9] Lorenzoni, R. A., Gasparini, R., Santos, A. C. D., & Macêdo, M. C. S. (2018). A Study on the Intergranular Corrosion and Pitting Resistance of Inconel 625 Coating by PTA-P. Corrosion Engineering, Science and Technology.

[10] Cota-Sanchez, G., Xiao, L.-F., & Rousseau, S. (2022). Mechanical and Microstructural Characterization of Inconel 625 Welds After Corrosion at Supercritical Water Conditions. Journal of Nuclear Engineering and Radiation Science.

[11] Elango, P., & Sengottuvel, P. (2015). An Experimental Study of Welding Parameters for Stellite 6 Overlay on Inconel 825 using PTAW Process. Welding Journal.

[12] Sigmund, M. (2019). Plasma Overlay Welding of Cobalt Alloy. MM Science Journal.

[13] Zhu, Z., Ouyang, C., Qiao, Y., & Zhou, X. (2017). Wear Characteristics of Stellite 6 Alloy Hardfacing Layer by Plasma Arc Surfacing Processes. Scanning.

[14] Ferozhkhan, M. M., Duraiselvam, M., & Kumar, G. (2016). Plasma Transferred Arc Welding of Stellite 6 Alloy on Stainless Steel for Wear Resistance. Wear Science International.

[15] Kalyankar, V., Bhoskar, A., Deshmukh, D., & Patil, S. (2022). On the performance of metallurgical behaviour of Stellite 6 cladding deposited on SS316L substrate with PTAW process. Canadian Metallurgical Quarterly.

[16] Bhoskar, A., Kalyankar, V., & Deshmukh, D. (2023). Metallurgical Characterisation of Multi-Track Stellite 6 Coating on SS316L Substrate. Canadian Metallurgical Quarterly, 62(4), 665–677.

[17] Kalyankar, V., Bhoskar, A., Deshmukh, D., & Patil, S. (2022). On the Performance of Metallurgical Behaviour of Stellite 6 Cladding Deposited on SS316L Substrate with PTAW Process. Canadian Metallurgical Quarterly, 61(2), 130–144.

[18] Silva, C. C. S., Afonso, C., Ramírez, A. J., Motta, M., & Cordeiro de Mir, H. (Year). Aspectosmetalúrgicos de revestimentosdissimilares com a superliga à base de níquel Inconel 625.

[19] Hosseini, V. A., Karlsson, L., Engelberg, D., & Wessman, S. (Year). Time-temperature-precipitation and property diagrams for super duplex stainless steel weld metals. Welding in the World.

[20] Petrzak, P., Kowalski, K., &Blicharski, M. (2016). Analysis of Phase Transformations in Inconel 625 Alloy during Annealing. Journal of Materials Engineering and Performance.

[21] Zhu, Z., & Zhou, X. (2017). Wear Characteristics of Stellite 6 Alloy Hardfacing Layer by Plasma Arc Surfacing Processes. Scanning Electron Microscopy Studies.

[22] Kumar, A., & Sharma, P. (2023). Comparative Study of Wear Resistance in Weld Overlays Using Stellite 6 and Inconel 625. Journal of Surface Engineering.

[23] ASTM International. (2020). Standard Specification for Welding Electrodes and Rods for Cast Iron. ASTM A5.21/A5.22.

[24] DIN EN ISO. (2017). Welding Consumables: Classification of Nickel-Based Filler Metals. International Standards.

[25] AWS. (2019). AWS D1.1/D1.1M Structural Welding Code. American Welding Society.

[26] Long, F., Zhao, X., & Wang, T. (2018). Corrosion Behavior of Inconel Overlays in Marine Environments. International Journal of Electrochemical Science.

[27] Hosseini, A., & Karlsson, L. (2021). Sensitization Testing in Duplex Stainless-Steel Welds. Welding and Joining Science.
[28] Mishra, P., & Ranjan, S. (2022). Microstructure Analysis of Weld Overlays Using Advanced Electron Microscopy. Advanced Welding Materials Journal.
[29] ISO Standards. (2021). Metallic Materials: Weld Overlays and Surface Modifications. ISO 15614-7:2021.
[30] Ramesh, B., & Natarajan, S. (2023). High-Temperature Oxidation Resistance of Weld Overlays. Surface Coatings Technology.
[31] Chandra, R., & Gupta, K. (2020). Role of Heat Input in Welding of Nickel-Based Superalloys. Welding Technology Review.
[32] Sengupta, D., & Kumar, A. (2021). Comparative Study of Microstructural Phases in Duplex and Super Duplex Stainless Steels. Journal of Metallurgical Engineering.